Maskless holographic schemes based on phase micromirror SLMs

Borisov, M., Chelubeev, D., Chernik, V., Merkushov, L., Rakhovskiy, V., et al.

M. Borisov, D. Chelubeev, V. Chernik, L. Merkushov, V. Rakhovskiy, A. Shamaev, "Maskless holographic schemes based on phase micromirror SLMs," Proc. SPIE 11324, Novel Patterning Technologies for Semiconductors, MEMS/NEMS and MOEMS 2020, 113241K (23 March 2020); doi: 10.1117/12.2552074

SPIE.

Event: SPIE Advanced Lithography, 2020, San Jose, California, United States

Maskless holographic schemes based on phase micromirror SLMs

M. Borisov, D. Chelubeev, V. Chernik, L. Merkushov, V. Rakhovskiy*, A. Shamaev
NANOTECH SWHL GmbH, Überlandstrasse 129, 8600 Dübendorf, Switzerland

ABSTRACT

We propose a scheme of maskless holography as a base of a novel lithographic technic. Maskless schemes based on reflective SLMs with planar and non-planar layouts are considered. Several effective methods of phase hologram synthesis adapted to the layouts are also introduced. These methods are based on the holographic lithography approach and calculation algorithms that have been developed by Nanotech SWHL. The aim of the work is to find the proper scheme and SLM characteristics, e.g. micromirror size, flatness, dynamic stability, etc. The non-flat optical schemes based on array of reflective SLMs will allow to achieve high NA up to 0.9 without immersion. That investigation allows to design a photolithographic tool with high diffraction efficiency and high-end capabilities.

Keywords: digital holography, dynamic hologram, holographic lithography, maskless lithography, dynamic mask

1. THE IDEA OF MASKLESS LITHOGRAPHY

Over the past fifteen years, Nanotech SWHL employees are developing methods of sub-wavelength holographic lithography. This new technology is an alternative to conventional lithography and based on the idea to replace a projection mask with a holographic mask. This technology has several important advantages over the projection lithography, among which it is necessary to highlight (1) the extreme stability of the reconstructed image to local defects occurred on a holographic mask; (2) a simple design of geometric pattern on a holographic mask, which is comprised of large (about the wavelength) and identical in shape transmittance zones; and (3) the absence projection imaging system between a mask and a wafer, the image in wafer reconstructs only due to diffraction between transmittance zones in free space without help of any lens. These promising properties of holographic lithography dramatically reduce the cost of mask manufacturing and their subsequent maintenance. The basic principles of the SWHL are described in more detail in [1–3] and our manuscript at this conference. They are based on the classic work of D. Gabor [4], where he proposed a method that enables a light field to be recorded in a medium and later reconstructed when the original light field is no longer present. Our works represent a significant development of digital holography methods resulted in the ability to reconstruct light images with billions of elements of sub-wavelength sizes on planar and even on non-planar wafers[5].

Holographic masks are manufactured with the same technologies as projection masks. Each mask is suitable only for obtaining one pattern and, in this sense, is disposable. During the work on the SWHL technology, the idea was raised to synthesize holographic masks for the so-called “maskless” or “dynamic” lithography, where the mask is replaced with a spatial light modulator (SLM) consisted of elements, which position or electromagnetic properties can be controlled. So SLM can adjust an incident electromagnetic wave in such a way that it would be possible to reconstruct a given light image with given accuracy and in the right place. In this case, masks are no longer required, which could radically simplify and reduce the cost of microelectronic production.

There are several works devoted to maskless lithography in the field of projection lithography of low resolutions [6–9]. In these works, a raster (point) image created with an SLM, for example, LCOS-SLM, is transferred by the projection lens to the wafer. The image resolution is limited to a pixel size and a pixel pitch of an SLM and the reducing magnitude of the projection system.

*rakhvi@nanotech-swhl.com; phone +41 79 583 19 57; nanotech-swhl.com

Novel Patterning Technologies for Semiconductors, MEMS/NEMS and MOEMS 2020,
edited by Martha I. Sanchez, Eric M. Panning, Proc. of SPIE Vol. 11324, 113241K
 · doi: 10.1117/12.2552074

Nowadays maskless lithography seems inapplicable in high-end projection lithography due to the following circumstances. The reducing magnitude of the projection system is in general no more than four times. The minimum size of an SLM pixel size is at least 2 μm. Therefore, the final resolution for a maskless projection system is limited to at least 0.5 μm. Moreover, the reconstruction image will turn out to be of poor quality, because widely used resolution enchantment techniques (RET), such optical proximity corrections (OPC) or sub-resolution assist features (SRAF), are inapplicable, while these corrections are usually of sub-wavelength size and cannot be translated to pixel-sized scale. Even if it could be possible to provide RET for maskless lithography the mask pattern will be reduced only by 5-10 times, that insufficient in high-end applications. There are proposals to develop a projection lens with a reduction of 100:1[10] or so and use the exposure technique in parts. However, the exposed size of a high-quality image with such reduction will not exceed 100 μm x 100 μm that leads to 10,000 exposures in the case of imaging 1 cm^2, which is obviously inappropriate.

2. SWHL MASKLESS HOLOGRAPHY

SWHL requires no projection lens. Moreover, there is no direct correspondence between mask feature sizes and the resolution of the reconstructed image, because hologram elements can be several times and even tens of times longer than the wavelength even for a sub-wavelength image. This remarkable feature was both theoretically and through simulations verified. So SWHL approach can be adapted to current SLM pixel size in both low- and high-end applications. Therefore, the idea of replacing a mask with an SLM is fundamentally unhindered in SWHL. It is only necessary to develop a program that provides us how to adjust positions or properties SLM pixels for the desired image.

Our company has developed efficient programs for the synthesis of amplitude holographic masks. This mask type reduces only an amplitude of a wave passing through a mask by a pre-calculated number of times. So, our algorithms synthesize a real-valued transmittance function $A(x)$, which values are in range 0-1. An output field for a wave $v(x)$ passed through the mask at point x is described as $A(x)$v(x). Designs of SLMs convenient for the maskless SWHL are piston Digital-Micromirrors Devices (DMD). Such devices can adjust, in contrast, only phase delays of the incident wave. We developed methods for converting amplitude hologram mask into a phase hologram mask, where a light image is formed only by phase delays for an incident wave.

Two ways of such a "conversion" can be distinguished.

The first is to replace the real-valued transmittance function of the amplitude hologram $A(x)$ with the function $exp[ikA(x)]$ taking imaginary values, where k is the real coefficient to be chosen. This method can be arbitrarily called the "whitening method" since the hologram of variable transmittance turns into a completely transparent one. There are known methods of such conversion by chemical means, described, for example, in Collier[11].

The second method is to group pixels of SLM into a "combined" macropixel [12], consisted of 2 x 2 ordinary pixels. So instead of modeling a phase transmittance function for a phase SLM, we model a complex transmittance function for combined micropixels. Then the complex value for each macropixel is translated into phase delays for its constituent pixels. Certain phase delays are formed in each macropixel so that due to interference, the total power of the wave transmitted through the cell is attenuated by the required number of times.

We carried out mathematical modeling of both the whitening method and the combined cell methods. Am SLM was simulated, consisting of approximately a million mirror elements located on a flat surface. The linear size of each mirror element was 8 μm. Each mirror element could move parallel to itself by a value of h, which could take 256 different values with a uniform pitch. Unfortunately, such a simple scheme for reflection from flat transparency does not allow us to obtain a numerical aperture of the optical path of more than 0.4; therefore, the resolution on the image was "wavelength", of the order of 1.5 of the wavelength of the radiation used. To obtain higher resolutions, you need to use other optical schemes with non-planar SLM, which will be discussed below. Our modeling, however, confirmed the fundamental feasibility of further implementation of holographic methods for dynamic (maskless) lithography.

In our research, undoubtedly, the question of the influence of the gaps between SLM pixels on the quality of the image, especially for non-planar optical schemes remains insufficiently studied. The following are various optical schemes of

maskless SWHL and some estimates for them. However, large-scale mathematical modeling with experimental verification is required to measure the quality of the reconstructed image. This is still expected to be implemented.

3. TYPES OF SLMs

SLMs can be divided by methods of operation into refractive and reflective.

By the method of adjustment of electromagnetic wave with a single pixel, SLMs can be divided into:

1. amplitude-only;

2. phase-only;

3. polarization - change the polarization of the wave;

4. complex and mixed – adjust several characteristics at once.

The difference between combined and mixed SLMs is that for a combined one the effect of changing several characteristics is planned, while for a mixed one it is inevitable.

According to the shape of the surface on which the SLM pixels are located, the SLM can be divided into planar and non-planar.

Below we consider samples of optical schematics with both planar and non-planar(ellipsoidal) dynamic mask. We analyze the possible geometries of these schematics. Spherical dynamic mask and parabolic one are not considered in the paper because our investigation demonstrate no sufficient profit from these masks compared to ellipsoidal mask. The only interesting feature of the parabolic mask is a possibility to use a parallel illumination beam.

4. SCHEME WITH REFLECTIVE PLANAR SLM

A planar reflective SLM must be placed in a converging spherical beam (Fig. 1). In this case, the photodetector is located on the side.

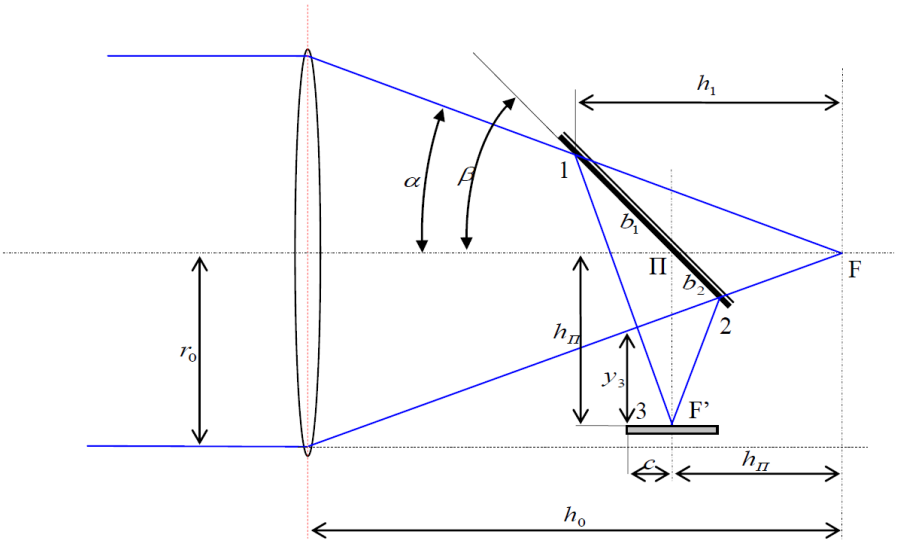

Figure 1. Scheme with planar reflective SLM

As shown in Figure 1, the system layout consists of a source a spherical converging wave of an angular aperture 2α, a reflective planar SLM (reflective holographic mask) of width $b = b_1 + b_2$, mounted at an angle β to the optical axis, and

a photodetector of width 2c, which should be located outside the incident light beam ($y_3 > 0$). The center of the holographic mask is located on the optical axis of the converging beam at the point Π at a distance $h_П$ from the focus point F of the illuminator. The maximum proximity of the mask to the objective is achieved when $h_1 = h_0 - \Delta h_k$, where Δh_k is the constructive clearance between the objective and the SLM. The holographic mask size is defined as

$$b = b_1 + b_2 = 2h_\Pi \frac{tg(\beta)}{cos\ (\beta)} \frac{tg(\alpha)}{tg^2(\beta) - tg^2(\alpha)} \tag{1}$$

The light aperture of the illuminator is calculated by the formula:

$$d_0 = 2r_0 = 2(h_1 + \Delta h_k)tg\alpha = b\ cos\ (\beta)\left(tg(\beta) + tg(\alpha)\right) + 2\Delta h_k tg\alpha \tag{2}$$

Numerical Aperture

The maximum numerical aperture depends on the position of the photodetector in the scheme:

1. Option A. When the photodetector is out of the parallel beam supplying the lens-former ($h_\Pi > r_0$), the resolving equation will be

$$\frac{\Delta h_k}{tg(\beta) - tg(\alpha) - tg(\beta)tg(\alpha)} = \frac{b\ cos\ (\beta)}{2} \cdot \frac{tg^2(\beta) - tg^2(\alpha)}{tg^2(\alpha)tg(\beta)} \tag{3}$$

Setting parameters Δh_k, β and b, it is possible to find the maximum angle α_{max} from this equation. The result is slightly dependent on the SLM size b (Table 1).

Table 1. Aperture and resolution depending on b whenever $\beta = 45°$ and $\Delta h_k = 5mm$

b, mm	Maximum numerical aperture $NA = sin\ (\alpha_{max})$	Resolution		Illuminator aperture $d_0 = 2r_0$, mm
		With 180° phase-contrast	Without phase-contrast	
13	0.395	0.6λ	1.4λ	17.44
260 = 20*13	0.44	0.525λ	1.2λ	279.90

2. Option B. When the photodetector is inside the parallel beam dimension but does not touch the conical beam boundary ($h_\Pi < r_0$, $y_3 > 0$), the resolving equation can be simplified to:

$$\frac{b}{2} cos\ (\beta)\left(tg^2(\beta) - tg^2(\alpha)\right)\left(1 - tg(\alpha)\right) = c \cdot tg^2(\alpha)tg(\beta) \tag{4}$$

The requirement of the closest proximity of the SLM to the lens, in this case, is not included in the calculation. The result is highly dependent on the ratio of b and c.

Table 2. Aperture and resolution depending on b whenever c = 15mm

b, mm	Maximum numerical aperture $NA = sin\ (\alpha_{max})$	Resolution		Illuminator aperture $d_0 = 2r_0$, mm
		With 180° phase-contrast	Without phase-contrast	
13	0.37	0.65λ	1.5λ	16.78
260 = 20*13	0.6	0.35λ	0.77λ	332.52

Thus, in the second case, a large numerical aperture is provided by a significant excess of the SLM width over the photodetector width.

Advantages and disadvantages

The proposed scheme is applicable to work with industrial wafer sizes (200-300 mm). Option A is most suitable, however, the numerical aperture is limited to 0.4-0.5.

Option B allows us to use larger numerical apertures than Option A, but it requires a small photodetector. The scheme is convenient for phase SLM. The utilization of amplitude SLMs is difficult. The introduction of immersion in the scheme is also difficult.

5. SCHEME WITH ELLIPSOIDAL REFLECTION SLM

The principle of operation is the following: a spherical diverging wave leaves the first focus of an elongated ellipsoid and diffracts on the inner surface of the ellipsoid, comprised of reflective SLMs. Then the zero-order diffraction concentrates in the second focus, and an aerial image is reconstructed in the specified plane near the second focus (Fig. 2).

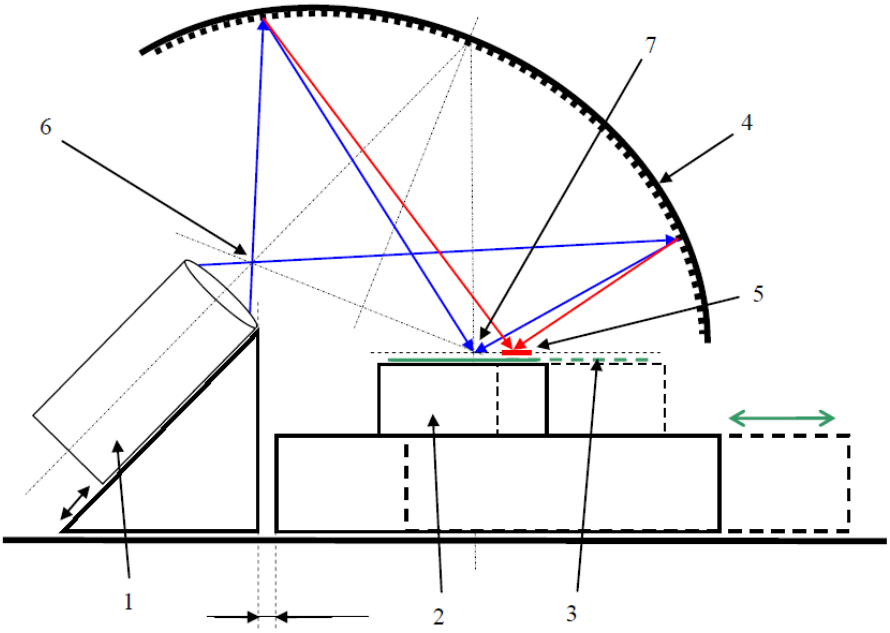

Figure 2. The scheme of ellipsoidal reflection SLM. 1 - Optics forming a spherical diverging wave; 2 - Movable bearing for a wafer; 3 - Wafer; 4 – Ellipsoidal SLM; 5 - Reconstructed image; 6, 7 – foci of the ellipsoid.

The required minimum distance between the foci of the ellipsoid is calculated based on dimensions of the illuminator, the movable bearing, the table, and the clearance *b*. The angular aperture is not structurally limited (Fig. 3).

Table 3. Calculation parameters

Symbol	Meaning	Constraints
F', F"	Foci	-
A	Major axis	$A \geq C + 2R$
B	Semi-minor axis	$B = \frac{1}{2}\sqrt{A^2 - C^2}$

C	Distance between foci (doubled focal distance)	$C \geq \frac{d}{2} + b + D - G$
R	Distance between focus and vertex	$R \geq L$, $L \approx \frac{smG}{\lambda}$, where m – binarization accuracy, λ - wavelength. Theoretical constraint $m \geq 2$, practical one $m = 2.5 - 5$
s	SLM pitch size	Manual
D	Dimensions of table for wafer	$D > D_W$, where D_W – wafer diameter
G	Image size – distance between focus and the most distant image point from the focus	Calculated by the given image size and its location relative to the focus
d	The horizontal dimension of the illuminator	Manual
b	Design margin of distance between the illuminator and the table	$b > 0$

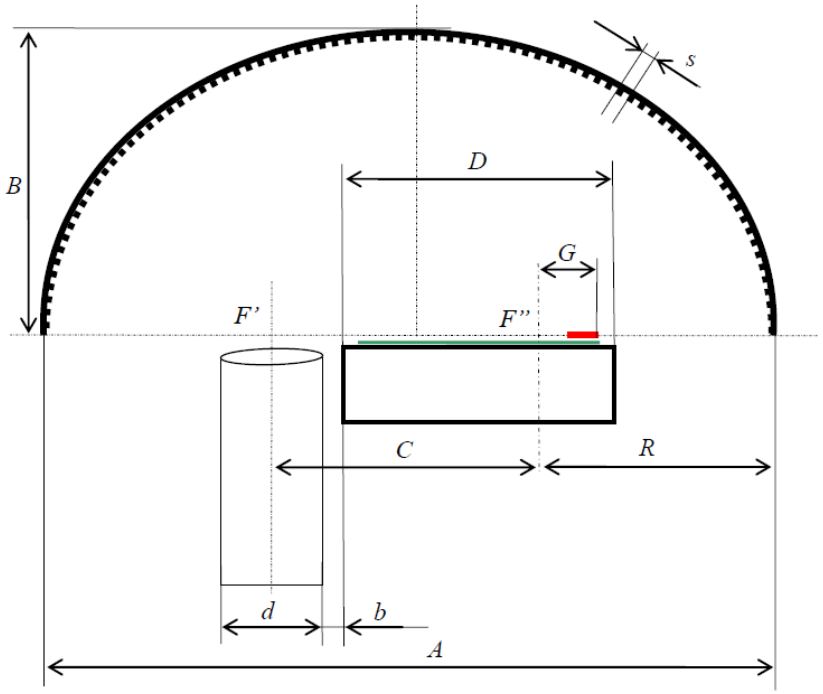

Figure 3. Main dimensions of the layout

The dimension of the cavity of the reflector in the cross-section does not exceed 2B. The following is a calculation of the key dimensions and characteristics of the proposed scheme conditioned by the operating parameters:

1. The reconstructed image has a size x = 26mm by y = 33mm, located relative to the focus, as shown in Fig. 4. The indent of the image from the focus is $G' = 3mm$.
2. Wavelength $\lambda = 365nm$.
3. SLM pixel pitch $s = 10\mu m$.
4. Binarization accuracy $m = 3$.

5. The horizontal size of the illuminator $d = 50mm$.
6. The distance between the illuminator and the table $b = 10mm$.
7. The diameter of the plate with photoresist $D_W = 300mm$, we accept table dimension $D = 320mm$.

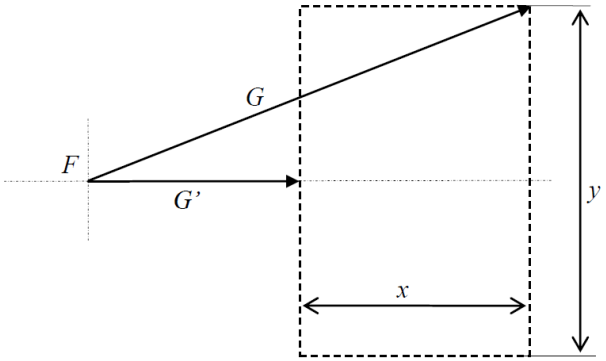

Figure 4. Dimensions and position of the image area

The previous parameters result in:

8. $G = 33.4mm \approx 34mm$
9. $R \geq \frac{smG}{\lambda} = \frac{10\mu m \cdot 3 \cdot 34mm}{0{,}365\mu m} = 2794.5mm \approx 2.8m.$
10. $\mathrm{C} \geq \frac{d}{2} + b + \mathrm{B} - G = \frac{50}{2} + 10 + 320 - 34 = 321mm.$
11. $A \geq C + 2R = 321 + 2 \cdot 3288 = 6897mm \approx 6.9m$
12. $B = \frac{1}{2}\sqrt{A^2 - C^2} = \frac{1}{2}\sqrt{6897^2 - 311^2} = 3444.8mm \approx 3.45m$

If the SLM pixel size is 2 μm, and the image size is 10 mm by 10 mm with the same indentation, the parameters become:

9. $R \geq \frac{smG}{\lambda} = \frac{2\mu m \cdot 3 \cdot 14mm}{0.365\mu m} = 230mm,$
10. $\mathrm{C} \geq \frac{d}{2} + b + \mathrm{B} - G = \frac{50}{2} + 10 + 320 - 14 = 341mm$
11. $A \geq C + 2R = 341 + 2 \cdot 230 = 801mm,$

$B = \frac{1}{2}\sqrt{A^2 - C^2} = \frac{1}{2}\sqrt{801^2 - 341^2} = 363mm.$

The angular and numerical aperture in the ellipsoidal reflection SLM are structurally and practically unlimited and can exceed 0.9.

Advantages and disadvantages

The numerical aperture can be made large enough, but it requires to create a source of a diverging spherical wave with a corresponding large radiation angle.

The scheme with an elliptical mirror is much more complicated in manufacturing, but it allows us to separate the light source from the photodetector, thus the scheme can utilize larger photodetectors.

The scheme is aimed to work with phase SLMs, the scheme has a poor adaptation to amplitude SLMs.

6. ADVANTAGES OF THE ELLIPSOIDAL DYNAMIC MASK

1. The numerical aperture is less limited compared to the planar scheme.

2. Higher rigidity of the ellipsoidal scaffold compared to a flat scaffold.

3. There is a simple way to control the accuracy of the basic shape - an elongated ellipsoid.

4. An introduction of metal coating on micromirrors allows working at any wavelength from a wide range of wavelengths reflected by this metal.

5. The relative simplicity of manufacturing for phase-shifting micromirrors a scaffold of ellipsoidal form with low geometric accuracy.

6. The simplicity of manufacturing an illuminator in case of low numerical apertures.

REFERENCES

[1] Borisov, M. V., Borovikov, V. A., Gavrikov, A. A., Knyaz'kov, D. Yu., Rakhovskii, V. I., Chelyubeev, D. A. and Shamaev, A. S., "Methods of the development and correction of the quality of holographic images of geometry objects with subwave-size elements," Doklady Physics 55(9), 436–440 (2010).

[2] Mikhail V. Borisov, Dmitriy A. Chelyubeev, Vitalij V. Chernik, Alexander A. Gavrikov, Dmitriy Yu. Knyazkov, Petr A. Mikheev, Vadim I. Rakhovsky and Alexey S. Shamaev., "Phase-shift at subwavelength holographic lithography (SWHL)," presented at Proc.SPIE, 16 April 2012.

[3] Borisov, M. V., Chelyubeev, D. A., Chernik, V. V., Gavrikov, A. A., Knyazkov, D. Yu., Mikheev, P. A., Rakhovsky, V. I. and Shamaev, A. S., "Phase-shift at subwavelength holographic lithography (SWHL)," presented at 28th European Mask and Lithography Conference (EMLC 2012), 17 January 2012, Dresden, Germany, 83520P.

[4] Gabor, D., "Holography, 1948-1971: Nobel Lecture," 11 December 1971, <https://www.nobelprize.org/prizes/physics/1971/gabor/lecture/> (20 January 2020).

[5] Chernik, V., Rakhovskii, V., Borisov, M., Chelyubeev, D., Miheev, P. and Shamaev, A., "Experimental verification of sub-wavelength holographic lithography physical concept for single exposure fabrication of complex structures on planar and nonplanar surfaces," Proc. SPIE 10446, 19, SPIE (2017).

[6] Totsu, K., Fujishiro, K., Tanaka, S. and Esashi, M., "Fabrication of three-dimensional microstructure using maskless gray-scale lithography," Sensors and Actuators A: Physical 130–131, 387–392 (2006).

[7] Zhong, K., Gao, Y., Li, F., Luo, N. and Zhang, W., "Fabrication of continuous relief micro-optic elements using real-time maskless lithography technique based on DMD," Optics & Laser Technology 56, 367–371 (2014).

[8] Ma, X., Kato, Y., van Kempen, F., Hirai, Y., Tsuchiya, T., van Keulen, F. and Tabata, O., "Experimental Study of Numerical Optimization for 3-D Microstructuring Using DMD-Based Grayscale Lithography," Journal of Microelectromechanical Systems 24(6), 1856–1867 (2015).

[9] Horiuchi, T., Koyama, S. and Kobayashi, H., "Simple maskless lithography tool with a desk-top size using a liquid-crystal-display projector," Microelectronic Engineering 141, 37–43 (2015).

[10] Chkhalo, N. I., Polkovnikov, V. N., Salashchenko, N. N. and Toropov, M. N., "Problems and prospects of maskless (B)EUV lithography," presented at The International Conference on Micro- and Nano-Electronics 2016, 30 December 2016, Zvenigorod, Russian Federation, 102241O.

[11] Collier, R. J., Burckhardt, C. B. and Lin, L. H., [Optical holography], Acad. Press, New York (1971).

[12] Arrizón, V., "Improved double-phase computer-generated holograms implemented with phase-modulation devices," Optics Letters 27(8), 595 (2002).